



# Revealing the capability of the European hake to cope with micro-litter environmental exposure and its inferred potential health impact in the NW Mediterranean Sea

Laura Muns-Pujadas<sup>a</sup>, Sara Dallarés<sup>a,\*</sup>, Maria Constenla<sup>a</sup>, Francesc Padrós<sup>a</sup>, Ester Carreras-Colom<sup>a</sup>, Michaël Grelaud<sup>b</sup>, Maite Carrassón<sup>a</sup>, Anna Soler-Membrives<sup>a</sup>

<sup>a</sup> Departament de Biologia Animal, Biologia Vegetal i Ecologia, Universitat Autònoma de Barcelona, Cerdanyola del Vallès, 08193, Barcelona, Spain

<sup>b</sup> Institut de Ciència i Tecnologia Ambientals (ICTA-UAB), Universitat Autònoma de Barcelona, Cerdanyola del Vallès, 08193, Barcelona, Spain

## ARTICLE INFO

### Keywords:

*Merluccius merluccius*  
Microplastics  
Anthropogenic items  
Fibre ingestion  
Cellulose  
Fish health  
Quality assurance  
Bioindicator

## ABSTRACT

Prevalence, abundance, concentration, size and composition of anthropogenic items (AIs) (synthetic and non-synthetic) ingested by *Merluccius merluccius* juvenile specimens and from near-bottom water samples from different localities off the Catalan coast (NW Mediterranean), were characterized. The potential effect of AIs on fish condition was assessed through different health indicators. Virtually all AIs found in fish and near-bottom water samples were fibres. A mean of 0.85 fibres/m<sup>3</sup> from the surrounding water was observed. Fish ingested a mean of 1.39 (SD = 1.39) items/individual. Cellulosic fibres were predominant (77.8% of samples), except for Barcelona. No differences in ingested AIs abundance and composition off Barcelona between 2007 and 2019 were found. Small AIs from the environment matched ingested AIs composition. Hakes did not ingest large fibres despite being present in the environment, probably due to their feeding behaviour. No adverse health effects or parasites aggregations were detected to be potentially related to AIs ingestion.

## 1. Introduction

For the last few decades, one of the topics that have generated considerable interest has been plastic litter and its potential impact on marine ecosystems. Presence of plastic pollution in surface waters was first reported in the 1970s (Carpenter and Smith, 1972). Since then, its occurrence has been detected throughout the marine ecosystem, resulting in research on the subject (Cole et al., 2011; Eriksen et al., 2014; Thompson, 2015; Gola et al., 2021). Many of these scientific studies deal with marine litter's impact on the environment and human activities all over the world (UNEP/MAP, 2015). This great interest stems from concerns about the global massive production of plastics. Even with ongoing efforts to reduce plastic use, almost 370 million tonnes of global plastics were still produced in 2019 (PlasticsEurope, 2021), and it is estimated that almost 60% of all plastics produced could reach the natural environment (Geyer et al., 2017). Due to their long environmental residence time and density, they can be vertically transferred down to the seafloor (Napper and Thompson, 2020) or horizontally transported by wind-driven circulation until being

concentrated in ocean gyres (van Sebille et al., 2020).

Originated by manufacturing or fragmentation of bigger plastic materials, plastic particles of less than 5 mm in diameter (i.e. microplastics (MPs), Arthur et al., 2009) are ubiquitous in the environment (Koelmans et al., 2022). Moreover, the presence of fibres with anthropogenic origin in the marine environment has also recently grown evidence (Suaría et al., 2020). In fact, it has been reported that as much as 80–90% of MPs in the marine environment correspond to fibres (Salvador Cesa et al., 2017). Some studies have tended to include the assessment of synthetic fibres (i.e. those composed of acrylic, polyester, polyamide, polypropylene, etc.) as a particular type of MPs (Salvador Cesa et al., 2017; Sanchez-Vidal et al., 2018). However, the great majority of fibres found in the oceans are non-synthetic fibres, composed of processed polymers from natural materials, for instance, regenerated cellulose and dyed cotton (Suaría et al., 2020). Indeed, several studies have evidenced the apparent dominance of both synthetic and non-synthetic textile fibres within the digestive tract of organisms (Taylor et al., 2016; Compa et al., 2018; Rodríguez-Romeu et al., 2020; Carreras-Colom et al., 2020). This hints that studies associated to

\* Corresponding author.

E-mail address: [sara.dallares@uab.cat](mailto:sara.dallares@uab.cat) (S. Dallarés).

<https://doi.org/10.1016/j.marenvres.2023.105921>

Received 11 November 2022; Received in revised form 10 January 2023; Accepted 15 February 2023

Available online 18 February 2023

0141-1136/© 2023 The Authors. Published by Elsevier Ltd. This is an open access article under the CC BY-NC-ND license (<http://creativecommons.org/licenses/by-nc-nd/4.0/>).

anthropogenic items (AIs) ingestion processes should include MPs and also pay special attention to the proportions of both synthetic and processed cellulosic fibres (Ryan et al., 2019).

In relation to marine litter accumulation, the Mediterranean Sea, which is a semi-enclosed basin, has become a hotspot for AIs (UNEP/-MAP, 2015) due to its particular hydrodynamics (Cózar et al., 2015), its densely populated coastal areas, high industrial and touristic activities, intense maritime traffic and the input of important rivers that are also strongly affected by human activities (e.g. Nile River, Po River). As a result of all these factors, abundance and distribution of micro-litter show high spatial heterogeneity along the Mediterranean (Simon-Sánchez et al., 2022). In the north-western Mediterranean Sea, AIs presence has been reported in different environments including coastlines (Llorca et al., 2020), surface waters (de Haan et al., 2019; Ryan et al., 2019), shallow seafloor sediments (Simon-Sánchez et al., 2022), deep-sea areas (Sanchez-Vidal et al., 2018) and also within the digestive tract of multiple organisms (Fossi et al., 2018), both benthic (Bellas et al., 2016; Carreras-Colom et al., 2018, 2020, 2022a, 2022b; Rodríguez-Romeu et al., 2020) and pelagic (Compa et al., 2018; Rodríguez-Romeu et al., 2022).

In this context, a common framework in European seas (Marine Strategy Framework Directive (MSFD, 2008/56/EC)) and in the Mediterranean Sea (IMAP, 2016) was developed, selecting specific marine species for monitoring spatial and temporal trends regarding marine litter pollution (Bellas et al., 2016; Fossi et al., 2018) for environmental risk assessment (Hermesen et al., 2018). This monitoring includes the presence of all kind and size of marine litter in geographical areas but also in ecosystems and organisms. In this sense, the European hake (*Merluccius merluccius* Linnaeus, 1758) has been recommended as a possible small-scale bioindicator species in FAO-GSAs due to its commercial and ecological importance (Fossi et al., 2018; Giani et al., 2019) and its wide distribution throughout the Mediterranean Sea (Oliver and Massutí, 1995). Moreover, owing to its benthopelagic feeding behaviour (Cartes et al., 2004) and since many of its preys move vertically with nictemeral rhythms, feeding takes place at different levels in the water column (Bozzano et al., 1997), so the hake may be exposed to AIs from the near-bottom environment as well as from the water column.

Researchers have reported a high heterogeneity in the prevalence of AIs ingestion by the European hake in the Mediterranean Sea (Giani et al., 2019; Mancuso et al., 2019; Bianchi et al., 2020; Avio et al., 2020). This high variability could be attributed to the presence of different concentrations of AIs in the different sampling areas and also to the bias induced by the lack of standardized methods and protocols for the assessment of the ingested AIs, thus hindering comparisons among studies (Lusher et al., 2017; Hermesen et al., 2018; Cowger et al., 2020). Surprisingly, none of these studies have related fish ingestion of AIs to the density and profile of AIs in the surrounding environment and, furthermore, none of them has assessed the potential effect of AIs ingestion on hake's health condition.

Although some studies carried out under laboratory conditions have shown that high levels of MPs ingestion can cause adverse effects due to the release of their associated toxic additives (Salvador Cesa et al., 2017), and that can interfere with feeding by causing gut blockages or lesions in the digestive system (Lusher et al., 2017; Kögel et al., 2020), there is no clear evidence of negative health effects derived from plastic ingestion in wild fish populations from areas with specific and real values of AIs in the environment (Rodríguez-Romeu et al., 2020, 2022).

Assessing an individual's health condition can be difficult due to the great variety of factors and elements of stress that may influence the physiological responses of the fish. For this reason, it is necessary to integrate different indicators into a multidisciplinary approach. In this context, condition indices can provide information on the overall health status which may be related to physiological or disease conditions. As general health indicators, these indices respond to an array of intrinsic and/or extrinsic factors including food availability, environmental variables, parasitism and anthropogenic factors (Lloret et al., 2014).

Fish parasite communities are widely used as indicators of fish health and environmental impact (Vidal-Martínez et al., 2010). Yet, few studies have examined parasites as bioindicators associated with the effect of AIs in fish (Rodríguez-Romeu et al., 2020, 2022; Pennino et al., 2020). The potential parasites-MPs relationships have been studied from different perspectives and particularly Hernandez-Milian et al. (2019) suggested that parasites aggregations in the intestine could favour the retention and accumulation of MPs, but other mechanisms could not be disregarded. At a much more detailed level, the use of histopathological techniques can help accurately detect alterations and pathologies in target organs. These alterations are robust health indicators and, in some cases, alterations can be associated to exposure to environmental contaminants (Au, 2004).

The present study aims to assess and characterize the presence of AIs ingested by *M. merluccius* in relation to the AIs present in the surrounding environment in the Balearic Sea, and to assess their potential impact on the health condition of these animals. To achieve this goal, prevalence, abundance, size and composition of AIs within the gastrointestinal tract of a representative sample of hake specimens captured in 2019 were determined from three different sampling areas that correspond to locations along the Catalan coast with different anthropogenic pressure levels. Environmental AIs (near-bottom water) were characterized in terms of abundance, concentration, size and composition and compared with those ingested in order to assess uptake by hakes. In order to assess the potential impact of AIs on *M. merluccius* health status, condition indices, histological alterations and parasite indicators were evaluated. Finally, potential changes in ingested AIs within a 12 years-gap were assessed, by comparing samples from the most polluted area collected in 2007 and in 2019.

## 2. Materials and methods

### 2.1. Study area and data collection

A total of 82 *M. merluccius* specimens were captured on board of commercial fishing trawlers at depths between 62 and 112 m on the continental shelf of the Catalan coast (NW Mediterranean) in the framework of the PLASMAR project (Spanish Ministry of Science, Innovation and Universities) and BIOMARE project (Spanish Ministry of Science and Innovation). In summer 2007, 20 specimens were collected off Barcelona while, in summer 2019, 62 hakes were collected from three different sites (Blanes, Barcelona and Ebro Delta coast) (Fig. 1; Table 1). Barcelona coast was selected as the most impacted area due to its important industrial activity, its densely populated coastline and its intense maritime transport (Tubau et al., 2015). Blanes coast was selected as considered a less impacted area owing to its lower industrial activity and sparse population compared to Barcelona. Ebro Delta coast was selected due to its particular characteristics, clearly different from Barcelona and Blanes coast. Ebro Delta is influenced by the Ebro River (910 km length, 14,000 hm<sup>3</sup>/y), which receives the inputs of both agricultural and industrial activities (Galimany et al., 2019).

Immediately upon capture, all individuals were fixed *in toto* in 10% buffered formalin, until further micro-debris analysis was developed. Environmental samples of near-bottom water were collected during fishing trawls in 2019 in order to ensure that they were taken in exactly the same surrounding environment as fish. The filtered material from water samples was collected using a WP2-net (200 µm mesh size), equipped with a mechanical flowmeter that was towed horizontally at a velocity of 2–3 knots and at 5–10 m above the seafloor along each trawl (ca. 30 min). Filtered water samples were immediately fixed in 10% buffered formalin until further processing (see below). ASTD152 CTD casts were performed at the same locations and 5 m above the seafloor prior to fishing trawls to record environmental variables (temperature, salinity, oxygen concentration and turbidity).

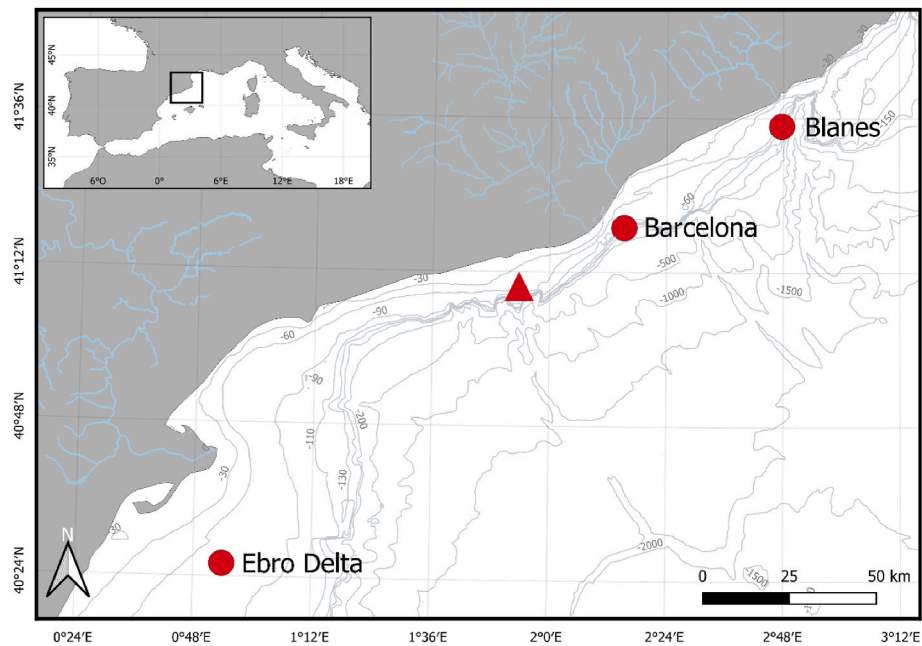


**Fig. 1.** Map of the study area. Red circles show the location of the three 2019 sampling points off Blanes at 111.5 m depth, Barcelona at 87 m depth and Ebro Delta at 65 m depth. Red triangle shows the location of the 2007 sampling point off Barcelona at 62.5 m depth.

**Table 1**

Biometric data, indices of fish health condition for each sampling point and the total of *Merluccius merluccius* examined (n) are shown. Mean and (standard deviation) were calculated for standard length (SL), total weight (TW), Le Cren relative condition index (Kn), hepatosomatic index (HSI) and stomach fullness (FULL). Significant differences among localities are indicated by different superscript letters.

| Location   | Year | Depth (m) | n  | SL (cm)      | TW (g)        | Kn                       | HSI                      | FULL        |
|------------|------|-----------|----|--------------|---------------|--------------------------|--------------------------|-------------|
| Blanes     | 2019 | 111.5     | 22 | 18.60 (0.02) | 70.20 (25.0)  | 1.01 (0.12) <sup>a</sup> | 2.68 (0.88) <sup>a</sup> | 1.91 (3.74) |
| Barcelona  | 2007 | 62.5      | 20 | 16.25 (1.13) | 43.10 (9.90)  | 0.97 (0.05)              | 2.22 (0.51)              | 3.44 (3.87) |
| Barcelona  | 2019 | 87        | 21 | 17.31 (1.35) | 54.34 (14.96) | 0.97 (0.06) <sup>a</sup> | 2.88 (0.74) <sup>a</sup> | 4.80 (5.35) |
| Ebro Delta | 2019 | 65        | 19 | 17.73 (2.55) | 65.82 (21.62) | 1.09 (0.11) <sup>b</sup> | 3.60 (1.12) <sup>b</sup> | 4.87 (3.80) |

## 2.2. Dissection procedure

At the laboratory, standard length (SL) and total weight (TW) were recorded for each specimen from 2007 and 2019. The visceral organs were removed and the liver (LW), gonads (GW) and stomach (SW) were weighed individually to the nearest mg. Then, the eviscerated weight (EW) of each specimen was recorded to the nearest g. Stomach, intestine and the rest of the organs (liver, gonads, spleen, heart, kidney and gills) were preserved in filtered 70% ethanol and stored separately for further analyses.

## 2.3. Visual inspection and collection of anthropogenic items (AIs)

### 2.3.1. AIs ingested by *M. merluccius* in 2007 and 2019

In order to recover AIs from the digestive tract, the stomach and intestine of each specimen were emptied, and their content was placed in separate glass Petri dishes. The screening of the gastrointestinal content was performed by visual inspection. Each AI found was cleaned, counted, individually mounted between glass slides in filtered distilled water and observed under the microscope for their characterization. A selection criterion adapted from Hidalgo-Ruz et al. (2012) for fibres was followed to prevent misidentification of AIs with organic material (e.g. seagrass or seaweed).

### 2.3.2. AIs from near-bottom water samples

In order to analyse the AIs from near-bottom water samples collected at the different sampling points, an aliquot of 100 mL of the homogenised mixture of fixed samples (0.5 L from samples off Blanes and

Barcelona and 0.8 L from samples off Ebro Delta) was filtered through a 1 mm mesh size stainless sieve into two fractions (>1 mm and <1 mm). Due to the huge amount of organic material, the <1 mm fraction was split into ten aliquots with a McLane rotary splitter (splitting error <4%). In order to prevent the degradation of cellulosic fibres (as explained by Carreras-Colom et al., 2022b), three of the ten aliquots were put together and exposed to a soft alkaline digestion (Cole et al., 2014): 20 mL of NaOH (1M) were added to the subsamples and left to react for 24h at room temperature. Subsamples were split again and two sub-aliquots were vacuum-filtered onto polycarbonate membranes (Millipore, Ø47mm, 0.45 µm mesh size). The filters were dried overnight at 40 °C and visually inspected for the presence of AIs. For the >1 mm fraction, AIs were directly picked from the stainless sieve under a stereomicroscope. After AIs extraction, all the concentrations obtained for the <1 mm fraction as for the >1 mm fraction were corrected in order to take into account all the splitting steps. AIs from both fractions were collected, counted and mounted individually between glass slides in filtered distilled water for their characterization.

## 2.4. AIs classification and analysis

After AIs isolation from all samples (hake's digestive contents from 2007 and 2019, and near-bottom water samples), images were taken at 50x to 400x of magnification and measures of mean diameter (calculated from three random measurements) and total length for fibres and mean cross-section (also from three random measurements) for fragments were recorded. Images and measurements were taken with a Leica camera model CTR5000 connected to a Leica DM500B microscope and

an image-processing software (ProgRes® C3). For each fish, number (nAI) and total length (TL) of AIs were calculated. Also, to infer the total length of AIs occupying the digestive system of fish, the sum of the lengths of all AIs (TLAI) found there was calculated for each specimen. Mean intensity of AIs was calculated as the mean number of AIs ingested per individual, excluding those without AIs. AIs were firstly classified into five different typologies (A to E, Table S1) according to the visual aspects of their morphology such as colour, length, cross-section, shape of the ends and characteristics and texture of the backbone (Zhu et al., 2019; Carreras-Colom et al., 2020; Rodríguez-Romeu et al., 2020).

Polymer composition of AIs >1 cm was identified by FTIR (Fourier-Transformed Infrared Spectrometry) using a Tensor 27 FTIR spectrometer (Bruker Optik GmbH, Germany) operating in Attenuated Total Reflectance (ATR) mode. Spectra was recorded as 16 scans in the spectral range of 600–4000  $\text{cm}^{-1}$  (Servei d'Anàlisi Química, Autonomous University of Barcelona). AIs <1 cm were chemically analysed by micro-FTIR using a Thermo Scientific™ Nicolet™ iN10 MX Infrared Imaging Microscope, and spectra was recorded as four scans in the spectral range of 800–4000  $\text{cm}^{-1}$  (CCitUB, University of Barcelona).

A randomly selected subsample of the AIs recovered from the digestive tract of hakes and from the environmental samples at each locality (at least 30% of the total AIs) were identified by micro-FTIR and FTIR spectroscopy. Likewise, all synthetic AIs (belonging to categories B, C, D and E), which by their morphological features were doubtful, were also analysed as well as a representative subsample of cellulosic-like AIs from category A in order to represent at least 10% of all cellulosic-like AIs found at each sampling point.

The resulting spectra were treated with Spectragryph 1.2.11 (Menges, 2021) in order to apply baseline corrections and select the spectral range of 800–3600  $\text{cm}^{-1}$ . Corrected spectra were compared with reference spectra (Primpke et al., 2018) and similarity correlation values > 70% were accepted for reliable identification. Correlation values ranging between 60 and 70% were also accepted only when their spectra matched visually with the reference and the visual appearance of the AI fitted with the description of the typology (Table S1). More than 80% of the spectra of all AIs analysed by micro-FTIR and FTIR corresponded to the assigned visual category.

## 2.5. Analysis of fish health condition in 2019

The general health condition of each fish was assessed through two physiological indices: Le Cren's relative body condition index ( $\text{Kn} = \text{EW}/(\alpha \times \text{SL}^\beta)$  (Le Cren, 1951), where Kn is the relative body condition,  $\alpha$  and  $\beta$  are the slope and the intercept of the weight-length relationship representing the entire dataset of sampled fish, and the hepatosomatic index ( $\text{HSI} = (\text{LW}/\text{EW}) \times 100$ ). The gonadosomatic index was not considered as all individuals were immature. Feeding intensity was calculated by the stomach-fullness index ( $\text{FULL} = (\text{CW}/\text{EW}) \times 100$ ), using the stomach content weight (CW) recorded after AIs inspection.

A portion of liver and digestive tract (stomach and intestine after AIs inspection) were embedded in paraffin and processed by routine histology techniques. The digestive tract was selected due to its direct contact with AIs and the liver was selected as a target organ for the assessment of potential changes associated to the presence of toxic additives within the AIs. All samples were sectioned at 5  $\mu\text{m}$  and stained with Haematoxylin and Eosin. Each sample was completely screened and qualitatively examined under the microscope for histopathological assessment and identification of specific disorders (e.g. inflammation, necrosis; see Kögel et al., 2020) which could be potentially related to the ingestion of AIs or their associated toxic substances, but not to detect the AIs themselves. Prevalence of histological alterations found in the samples was recorded for each fish. A random subsample of 10 fish per locality was used to determine the intensity of rodlet cells (RC) through a semi-quantitative analysis from histological sections of the stomach mucosa. RC were considered as their increase in number is related to exposure to physical and chemical injuries (Manera and Dezfuli, 2004),

and their presumed relationship to MPs exposure was suggested by Pedà et al. (2016). Three fields of view were randomly selected and counts of the number of rodlet cells were performed on each section at 400x of magnification, and scored according to cluster partitioning around medoids (PAM) as: low (1) (<11 RC per observation field), medium (2) (12–16 RC per observation field) and high (3) (>17 RC per observation field). Mean intensity was calculated from the average intensity values of each individual.

Fish external surfaces and right-side gills were inspected macroscopically for ectoparasites, and the rest of organs were checked for endoparasites under a stereomicroscope. All parasites found were counted, identified to the main taxonomic group and stored in 70% ethanol. For identification, platyhelminths and acanthocephalans were stained with iron acetocarmine, dehydrated through a graded ethanol series, cleared in clove oil and examined as permanent mounts in Canada balsam. Nematodes were cleared and examined as semi-permanent mounts in glycerine.

## 2.6. Quality assurance and quality control

In order to prevent airborne contamination, the dissection of all fish was performed in a laminar flow cabinet. Moreover, all dissection material and vials were rinsed three times with filtered distilled water (50  $\mu\text{m}$  metal sieve) before use, and nitrile gloves and cotton lab coat were used at all times.

Water samples processing was performed in a clean laboratory, consisting in an 8  $\text{m}^2$  hardwall laminar flow chamber ventilated through 4 laminar flow HEPA filters (H14). All material was previously rinsed and distinctive orange lab coats were used at all times. Procedural blanks were performed to check for potential contamination, and a mean of 0.63 fibres/blank were found. No fibres matching with the coloured coat were detected attributable to airborne contamination.

AIs screening of the gastrointestinal content and environmental samples was carried out inside an isolation device adapted from the one proposed by Torre et al. (2016), which consisted of a plastic cover isolating the binocular stereomicroscope and the work area from the surrounding environment. Moreover, dissection tools and Petri dishes used were rinsed with filtered distilled water before the examination of each sample. The gastrointestinal content of each specimen was diluted in more than one Petri dish when necessary and checked several times in the stereomicroscope to perform a complete inspection of the content and isolate all the AIs present in the samples. Procedural controls (Petri dishes containing a few ml of filtered distilled water) were placed inside and outside of the isolation device to assess the intensity of background airborne contamination during screenings (Bellas et al., 2016). As an outcome, contamination found in the outside controls was on average 5.1 times higher than contamination in the inside controls (average values of 0.19 fibres per digestive sample screened), thus demonstrating the effectiveness of the isolation device. Contamination in both controls consisted of fibres that always appeared on the surface of the water, indicating that they were deposited from the air. As a result of this observation, fibres found in the examined samples were only counted if they were clearly embedded in the digestive content. Thus, no correction factor was applied to the final values of the AIs obtained.

## 2.7. Data analysis

All variables were tested for normality and homoscedasticity using the Shapiro-Wilk test and the Levene's test, respectively. Data distribution was also plotted for visual assessment.

Fibres from the digestive tract and from the environment were classified into four size clusters by PAM applying the k-medoids algorithm on a matrix of dissimilarity. Likewise, RC intensity was also classified into three clusters by PAM. Each cluster was represented by one object which is located at its centre. The k clusters are established by assigning each object of the dataset to the nearest of the central objects,

thus objects that show a high level of similarity are grouped together, while objects which are most dissimilar are assigned to different clusters (Kaufman and Rousseeuw, 1990). In order to assess differences among sampled localities and between years (in the case off Barcelona) and organs as well as between fish and environmental samples in fibres size clusters proportions and AIs typologies, Chi-Squared or Fisher-exact tests (when sample size was too small) were applied. Also, Fisher-exact tests were used to detect differences in RC categories among localities. When significant differences were detected, pairwise tests were performed to determine which pairs of categories contributed to the overall significance. Differences in TL of fibres from water samples among localities were tested using Kruskal-Wallis test.

Differences among localities and between years (for samples from off Barcelona) on biological data (SL and FULL) and condition indices (Kn and HSI) were tested using Kruskal-Wallis and ANOVA tests, respectively. Post-hoc pairwise comparisons were carried out using Dunn's multiple comparison test for non-parametric data and TukeyHSD post-hoc tests for parametric data.

To assess differences in prevalence, mean abundance, mean intensity, TLAI and TL of synthetic and non-synthetic AIs among localities and organs (stomach/intestine), Generalized Linear Models (GZMs) (logistic model for prevalence and negative binomial model for mean abundance, mean intensity, TL and TLAI) were used, with SL and FULL set as covariates. Parasite prevalence (P) and mean abundance (MA) for each locality were calculated according to Bush et al. (1997) for the total of parasites recovered, for each major taxonomic group and only considering parasites within the digestive tract. GZMs were performed to test differences in P and MA of digestive parasites among localities (logistic model for prevalence and negative binomial model for mean abundance). Possible correlations between AIs (nAI and TLAI) and prevalence of histological alterations (i.e. granulomas, inflammation areas) were tested using GZMs (binary logistic model).

A correlation matrix was built in order to test possible associations of AIs descriptors (nAI, TLAI and TL), RC and parasite abundance with fish health condition indices (Kn and HSI) and FULL by means of Pearson's and Spearman's correlation tests.

Finally, a Multiple Factor Analysis (MFA) was used to simultaneously assess the relationship among AIs parameters, abundance of main parasite groups found in the digestive tract, environmental variables and fish health condition indices, and to visualize and differentiate groups of samples according to these variables. This multivariate analysis enables analysing and visualizing individuals that are characterized by different sets of variables (both quantitative and qualitative) which are structured into groups. Thus, the differences within groups are minimized whilst differences among groups are maximized.

Data analysis was performed using RStudio software, version 4.1.2, and using the PAMK function implemented in the package "fpc", the packages "dunn.test", "Hmisc", "FactoMineR" and "factoextra". Statistical significance was set at 0.05.

### 3. Results

#### 3.1. AIs ingested by *M. merluccius* in 2007 and 2019

A total of 41 of the 62 hakes from 2019 analysed contained AIs in their digestive tracts. A significant major prevalence of AIs was noticed off Blanes (90.9%), followed by Ebro Delta (63.1%) and Barcelona (42.8%) (GZM,  $\chi^2 = 10.289$ ,  $p = 0.006$ ). A total of 95 AIs were found within the digestive tracts of *M. merluccius*. The vast majority of AIs were fibres (97.8% of the total). Only one fragment (0.03 mm<sup>2</sup>) and one film (2 mm<sup>2</sup>) were detected in the intestine of two different individuals in Barcelona and Blanes, respectively. The mean number of AIs found per individual (nAI) was 1.39 (SD = 1.39) and the mean intensity of AIs per individual was 2.13 (SD = 1.18). The average length of the fibres (TL) found was 1.56 (SD = 1.24) mm, their mean diameter was 0.03 (SD = 0.07) mm and the mean sum of the total length of the AIs found per

individual (TLAI) was 3.43 (SD = 2.67) mm.

No differences of nAI, mean intensity or TLAIs were observed between stomach and intestine ( $p > 0.05$ ). Blanes was the location with the highest prevalence of non-synthetic AIs (GZM,  $\chi^2 = 15.314$ ,  $p = 0.003$ ) and mean abundance of both synthetic (GZM,  $\chi^2 = 6.388$ ,  $p = 0.03$ ) and non-synthetic (GZM,  $\chi^2 = 8.121$ ,  $p = 0.03$ ), and global AIs (GZM,  $\chi^2 = 7.247$ ,  $p = 0.03$ ) (Table 2). No significant differences among localities were found for the values of mean intensity, TLAIs and TL of either synthetic or non-synthetic AIs (GZM,  $p > 0.05$ ) (Table 2).

A total of 7 of the 20 hakes off Barcelona from 2007 analysed contained AIs in their digestive tracts. A total of 13 AIs were found within their digestive tracts. No significant differences in terms of prevalence, TLAIs, mean abundance, intensity and length of ingested AIs were found between 2007 and 2019 in Barcelona.

#### 3.2. Environmental water samples

A total of 180 AIs were found in near-bottom water samples. This is equivalent to an overall average concentration of 0.85 AIs/m<sup>3</sup> (0.52 AIs/m<sup>3</sup> off Blanes, 1.53 AIs/m<sup>3</sup> off Barcelona and 0.50 AIs/m<sup>3</sup> off Ebro Delta) (Table 2). All AIs detected in environmental samples were fibres. The average length of these fibres (TL) was 14.65 (SD = 14.29) mm and the mean diameter was 0.02 (SD = 0.004) mm. Significant higher values of the mean length of synthetic fibres from off Barcelona were detected compared to the other localities (K-W,  $\chi^2 = 26.15$ ,  $p < 0.01$ ) (Table 2).

Values of abiotic conditions (temperature, turbidity, salinity and oxygen concentration) of the near-bottom water layer from each locality are given in Table S2.

#### 3.3. AIs size classification

Fibres were classified into four different classes based on the PAM algorithm: small ( $\leq 1.15$  mm), medium (1.16–2.62 mm), large (2.63–6.39 mm) and extra-large ( $\geq 6.40$  mm). The most abundant size category within the digestive tracts of hakes was small (46.2%), followed by medium (39.8%) and the less abundant size category was large (14%). No extra-large fibres were found in fish samples. No significant differences in the size of the fibres ingested by hakes were found among localities nor between organs and years (Chi-squared,  $p > 0.05$ ). In near-bottom water samples, small was the most abundant fibre size class off Blanes (55.6%) and Ebro Delta (48.5%), contrary to Barcelona, where the most abundant size class was extra-large (79.1%). In this case, significant differences in the size of the fibres from water samples were found among localities (Chi-squared,  $\chi^2 = 73.86$ ,  $p < 0.001$ ). Fibre size distribution from water samples was significantly different to that of fibres ingested by hakes in Barcelona (Chi-squared,  $\chi^2 = 11.79$ ,  $p = 0.008$ ), but not in the case of the other localities (Fig. 2, Table S3).

#### 3.4. AIs polymer characterization

The 100% of the resulting spectrums from AIs belonging to category A were identified as cellulose. From category B, 86.3% of the spectrums were identified as polyethylene terephthalate (PET), 9.1% as polyamide and 4.5% as cellulose. In the case of category C, 100% of the resulting spectra corresponded to acrylic. Regarding category D, 96.2% of the resulting spectra matched to polyamide (PA) and 3.8% to PET. Finally, 75% of the resulting spectra from AIs belonging to typology E were identified as polypropylene (PP) and 25% as PET (Fig. 3).

Of the 108 AIs found in the hake's digestive tract in 2007 and 2019, cellulose was the most frequent polymer in all localities (overall prevalence 71.3%). The rest of the AIs were of synthetic composition, mostly PET (overall prevalence ca. 20%), but also acrylic and polypropylene. No significant differences among localities nor years were noticed in terms of polymer composition (Chi-squared,  $p > 0.05$ ).

Regarding the 180 AIs found in near-bottom water samples, cellulose was the most frequent polymer in Blanes and Ebro Delta. However,

**Table 2**

Prevalence of AIs ingested by fish and mean (standard deviation, SD) of the abundance, intensity, sum of total lengths (TLAI) and total length (TL) of the AIs (synthetic and non-synthetic) found in digestive contents of hakes in 2007 and 2019, as well as mean (SD) of the abundance, TLAI and TL in water samples, from each sampled locality in 2019. Different superscript letters indicate significant differences among localities.

| Digestive content                  | Year<br>n     | Blanes<br>2019<br>22     | Barcelona<br>2019<br>21    | 2007<br>20  | Ebro Delta<br>2019<br>19 | Total<br>2019 |
|------------------------------------|---------------|--------------------------|----------------------------|-------------|--------------------------|---------------|
| Prevalence (%)                     | Synthetic     | 40.91                    | 14.28                      | 10.00       | 21.05                    | 25.80         |
|                                    | Non-synthetic | 86.36 <sup>b</sup>       | 38.09 <sup>a</sup>         | 35.00       | 57.89 <sup>a</sup>       | 61.29         |
| Mean abundance (n/ind)             | Synthetic     | 0.60 (0.85) <sup>b</sup> | 0.14 (0.36) <sup>a</sup>   | 0.15 (0.49) | 0.26 (0.56) <sup>a</sup> | 0.34 (0.65)   |
|                                    | Non-synthetic | 1.50 (1.14) <sup>b</sup> | 0.52 (0.75) <sup>a</sup>   | 0.50 (0.76) | 1.11 (1.41) <sup>a</sup> | 1.05 (1.18)   |
| Mean intensity (n/ind)             | Synthetic     | 1.44 (0.73)              | 1.00 (0.00)                | 1.50 (0.71) | 1.25 (0.50)              | 1.31 (0.60)   |
|                                    | Non-synthetic | 1.74 (1.05)              | 1.38 (0.52)                | 1.43 (0.53) | 2.22 (1.20)              | 1.78 (1.02)   |
| TLAI (mm/ind)                      | Synthetic     | 3.78 (2.54)              | 1.37 (0.66)                | 2.29        | 2.99 (2.99)              | 2.71 (2.52)   |
|                                    | Non-synthetic | 2.41 (1.97)              | 1.52 (1.07)                | 1.43 (0.95) | 2.99 (2.22)              | 2.36 (1.91)   |
| TL (mm/ind)                        | Synthetic     | 2.54 (1.29)              | 1.37 (0.66)                | 1.15        | 2.11 (1.58)              | 2.27 (1.30)   |
|                                    | Non-synthetic | 1.34 (0.84)              | 1.35 (1.16)                | 0.87 (0.37) | 1.32 (0.69)              | 1.34 (0.87)   |
| <b>Environmental samples</b>       | <b>n</b>      | <b>1</b>                 | <b>1</b>                   |             | <b>1</b>                 |               |
| Mean Abundance (n/m <sup>3</sup> ) | Synthetic     | 0.21                     | 1.33                       |             | 0.06                     | 0.53          |
|                                    | Non-synthetic | 0.31                     | 0.19                       |             | 0.44                     | 0.32          |
| TLAI (mm/m <sup>3</sup> )          | Synthetic     | 0.07                     | 0.27                       |             | 0.11                     | 0.15          |
|                                    | Non-synthetic | 0.12                     | 0.03                       |             | 0.05                     | 0.07          |
| TL (mm/AI)                         | Synthetic     | 1.25 (0.49) <sup>a</sup> | 22.40 (12.92) <sup>b</sup> |             | 6.58 (5.63) <sup>a</sup> | 20.68 (13.56) |
|                                    | Non-synthetic | 2.00 (1.76)              | 1.34 (0.99)                |             | 1.60 (1.13)              | 1.66 (1.30)   |

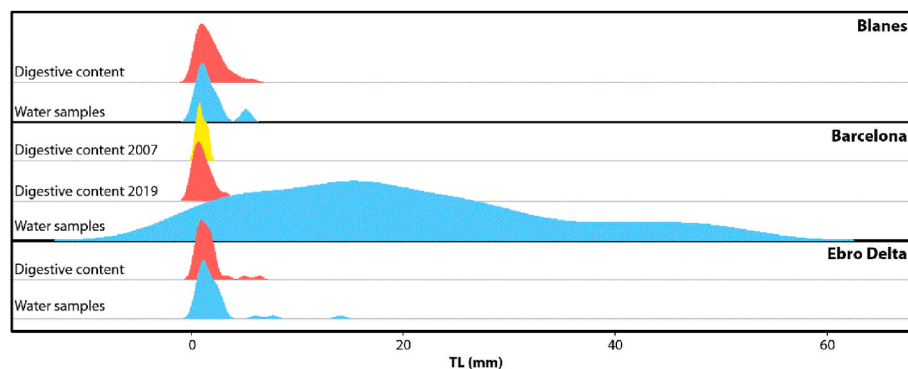


**Fig. 2.** Density standardized charts showing the distribution of the total length (TL, mm) of fibres from the digestive tract of *Merluccius merluccius* in 2019 (red colour), 2007 (yellow colour) and from near-bottom water samples (blue colour) according to the sampled locality.

polyamide fibres were predominant in Barcelona. In this case, significant differences were found in polymer composition among localities (Chi-squared,  $\chi^2 = 134$ ,  $p < 0.001$ ).

Composition of the AIs found in near-bottom water samples was significantly different from that of the AIs ingested by hakes in Barcelona (Chi-squared,  $\chi^2 = 97.8$ ,  $p < 0.001$ ) (Fig. 4).

### 3.5. Trends on fish biological parameters, histopathology and parasitological indicators

SL of the individuals examined ranged between 14.5 and 24.6 cm and no significant differences were found among localities nor between years ( $p > 0.05$ ). Fish from off Ebro Delta presented significantly higher values of Kn (ANOVA,  $F_{(79, 2)} = 10.575$ ,  $p < 0.001$ ) and HSI (ANOVA,  $F_{(59, 2)} = 4.915$ ,  $p < 0.001$ ). No significant differences among localities nor between years were detected regarding stomach fullness ( $p > 0.05$ ) (Table 1).

A total of 208 parasites were found in hakes of 2019. High total prevalence values were detected in all localities: 100% off Barcelona, 86.4% off Blanes and 94.7% off Ebro Delta. Among the most frequently found parasite groups, nematodes were the most abundant taxon, followed by digeneans and cestodes, and the least abundant groups were monogeneans and copepods (Table 3). A single isopod and one acanthocephalan were detected in two different individuals from Blanes and Ebro Delta, respectively.

No significant differences among localities were found for parasite total prevalence and mean abundance, either considering the total parasite load or only digestive parasites. However, a higher prevalence of cestodes (GZM,  $\chi^2 = 8.424$ ,  $p = 0.05$ ) and a higher abundance of digeneans (GZM,  $\chi^2 = 6.424$ ,  $p = 0.03$ ) were detected off Barcelona, and a significantly lower prevalence of digeneans was observed off Blanes (GZM,  $\chi^2 = 6.404$ ,  $p = 0.008$ ) (Table 3).

Histopathological analyses did not reveal alterations in the mucosa of the stomach or the intestine potentially associated to AIs abrasion. However, a particular high number of RC in the stomach mucosa and some granulomas were detected. No significant differences in RC intensity and prevalence of granulomas were detected among localities. Findings and changes observed in the histopathologic evaluation of the liver consisted of lipidic metamorphosis, granulomas, macrophages aggregates and presence of small inflammation areas, as well as contained degraded forms of nematodes larvae (Table 3). However, none of them could be related to AIs ingestion since no clear statistical relationships were found between the prevalence of these observations and the levels of AIs ingested by individuals (GZM,  $p > 0.05$ ).

The correlation matrix indicated no clear relationships among fish condition indices, stomach fullness, AIs parameters, parasite and RC abundance. General AIs parameters (abundance, sum of lengths and mean length) were positively correlated among them ( $\rho > 0.6$ ), with abundance and sum of length of cellulosic fibres (i.e. non-synthetic) showing high correlation values with total AIs abundance ( $\rho = 0.93$ ,

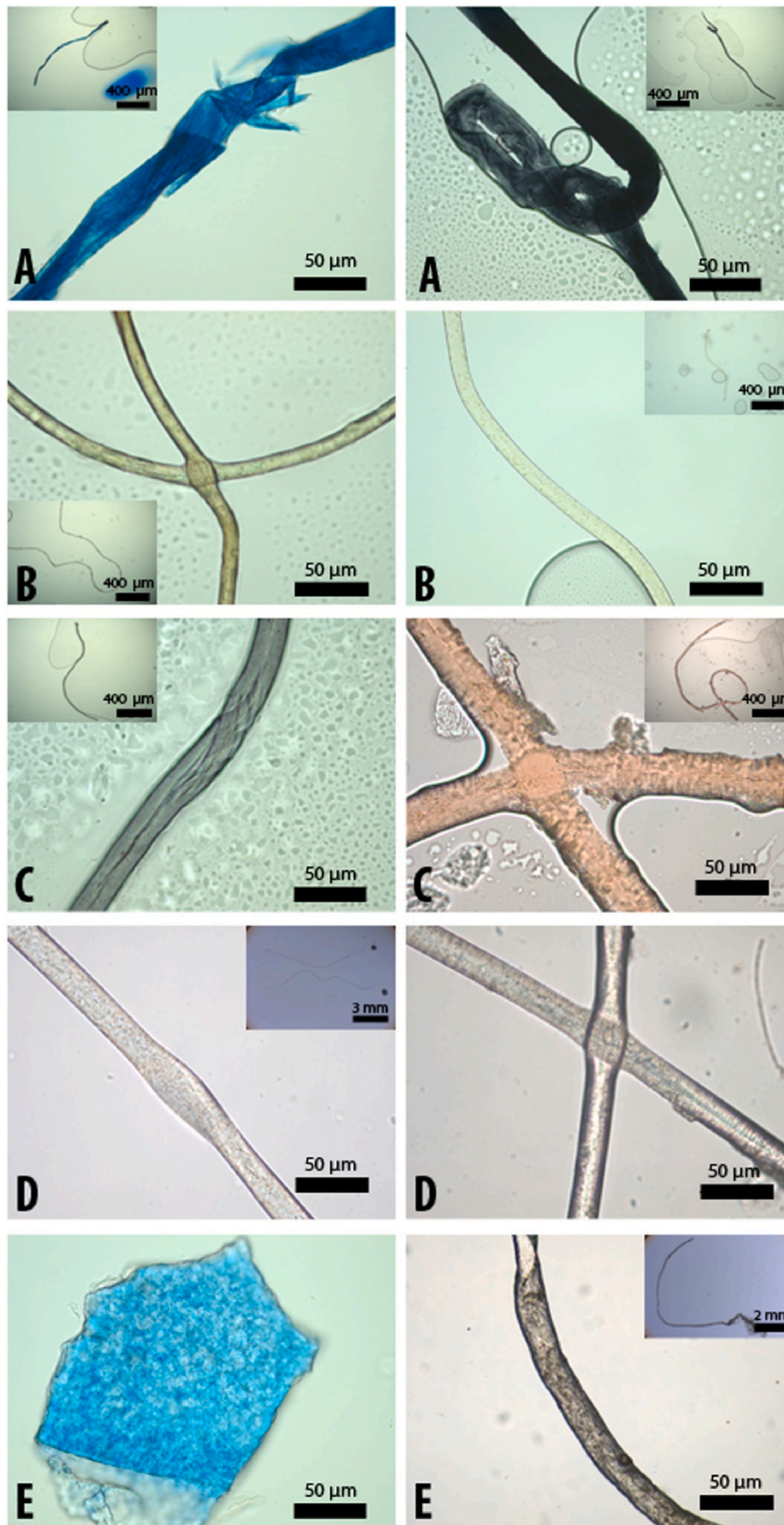


Fig. 3. Images of representative AIs of the five different typologies of polymers found in the digestive tract of *Merluccius merluccius* and in the surrounding near-bottom water samples. Each category (A to E) is described in Table S1.

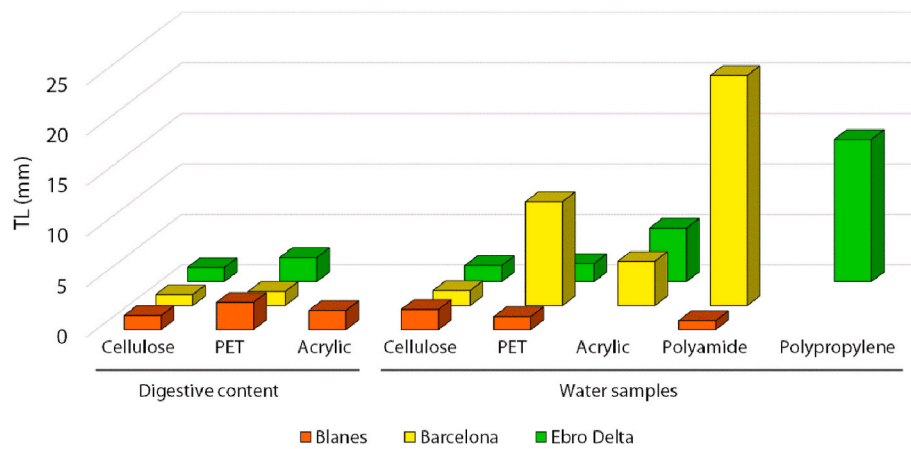


Fig. 4. Mean size (TL) and polymer composition of the AIs found in the digestive content of *Merluccius merluccius* and in water samples from each sampling area: off Blanes, off Barcelona and off Ebro Delta.

Table 3

Parasite descriptors and histopathological alterations found in *Merluccius merluccius* from each locality in 2019. Location within host and prevalence (P%) of main parasite taxa and histopathological alterations are shown. Mean abundance (MA) for parasite taxa and mean intensity (MI) for rodlet cells, followed by standard deviation (SD), are also displayed. Keys for locations within hosts: DT, digestive tract; G, gills; H, heart; L, liver; M, mesentery; S, stomach. In the case of Nematoda, Digenea and total parasites, total values and only the values from the DT are shown. Different superscript numbers and letters indicate significant differences in P% and MA, respectively, among localities. Only significant differences are indicated.

| PARASITE GROUP                       | Location          | Blanes P% | MA (SD)            | Barcelona P%             | MA (SD)            | Ebro Delta P%            | MA (SD)            | Total P%                 | MA (SD)        |             |
|--------------------------------------|-------------------|-----------|--------------------|--------------------------|--------------------|--------------------------|--------------------|--------------------------|----------------|-------------|
| <b>NEMATODA</b>                      | DT, L, M          | 54.55     | 0.95 (1.11)        | 61.90                    | 0.95 (0.94)        | 78.95                    | 1.63 (1.50)        | 64.52                    | 1.16 (1.22)    |             |
|                                      | DT                | 40.90     | 0.68 (0.99)        | 61.90                    | 0.95 (0.97)        | 73.68                    | 1.47 (1.50)        | 58.06                    | 1.02 (1.19)    |             |
| <b>PLATYHELMINTHES</b>               | <b>Digenea</b>    | DT, H     | 22.72              | 0.68 (1.43)              | 52.38              | 1.33 (1.71)              | 57.89              | 1.21 (1.72)              | 45.16          | 1.06 (1.62) |
|                                      |                   | DT        | 9.09 <sup>1</sup>  | 0.32 (1.13) <sup>a</sup> | 52.38 <sup>2</sup> | 1.33 (1.71) <sup>b</sup> | 42.10 <sup>2</sup> | 0.79 (1.32) <sup>a</sup> | 33.87          | 0.81 (1.45) |
|                                      | <b>Monogenea</b>  | G         | 4.55               | 0.04 (0.21)              | 14.29              | 0.14 (0.36)              | 5.26               | 0.05 (0.22)              | 8.06           | 0.08 (0.27) |
|                                      | <b>Cestoda</b>    | DT        | 45.45 <sup>1</sup> | 0.57 (0.67)              | 71.43 <sup>2</sup> | 1.00 (0.77)              | 26.32 <sup>1</sup> | 0.26 (0.45)              | 50.00          | 0.60 (0.69) |
|                                      | <b>ARTHROPODA</b> |           |                    |                          |                    |                          |                    |                          |                |             |
| <b>Copepoda</b>                      | G                 | 9.09      | 0.18 (1.41)        | 9.52                     | 0.09 (0.28)        | –                        | –                  | 6.45                     | 0.09 (1.15)    |             |
| <b>TOTAL</b>                         | DT, G, H, L, M    | 94.74     | 3.09 (3.05)        | 100.00                   | 3.76 (2.60)        | 86.36                    | 3.21 (2.34)        |                          |                |             |
|                                      | DT                | 81.81     | 2.00 (2.39)        | 95.24                    | 3.29 (2.10)        | 84.21                    | 2.58 (2.41)        |                          |                |             |
| <b>HISTOPATHOLOGICAL ALTERATIONS</b> |                   | <b>P%</b> | <b>MI (SD)</b>     | <b>P%</b>                | <b>MI (SD)</b>     | <b>P%</b>                | <b>MI (SD)</b>     | <b>P%</b>                | <b>MI (SD)</b> |             |
| <b>Lipid metamorphosis</b>           | L                 | 59.09     |                    | 47.61                    |                    | 68.42                    |                    | 58.06                    |                |             |
| <b>Granuloma</b>                     | L, S              | 45.45     |                    | 38.09                    |                    | 47.37                    |                    | 43.54                    |                |             |
| <b>Macrophages aggregates</b>        | L                 | 4.54      |                    | 4.76                     |                    | 5.26                     |                    | 4.84                     |                |             |
| <b>Inflammatory focus</b>            | L                 | 13.63     |                    | 9.52                     |                    | 15.78                    |                    | 12.90                    |                |             |
| <b>Rodlet cells (RC)</b>             | S                 | 90.00     | 1.70 (0.95)        | 100.00                   | 1.60 (0.84)        | 100.00                   | 2.10 (0.88)        | 98.38                    | 1.80 (0.89)    |             |

$p < 0.001$  and  $\rho = 0.92$ ,  $p < 0.001$ ), respectively. Mean length of synthetic AIs displayed high correlation values with mean total AIs length ( $\rho = 0.82$ ,  $p < 0.001$ ) (Fig. 5).

The MFA explained 36.2% of the variability by the two first axes. A differentiation was detected among fish from the three localities, as shown in Fig. 6B. The variables that explained most of the variability along the first dimension were the abundance of non-synthetic fibres ingested and abiotic parameters. Individuals off Blanes were characterized by a larger body size and higher AIs abundance (Fig. 6A). Regarding the second axis, specimens off Barcelona were related to higher abundance of cestodes and to temperature, and those off Ebro Delta were characterized mainly by the condition factor, abundance of nematodes, oxygen concentration and stomach fullness. Overall, abiotic conditions were the group of variables that contributed most to explain the model (Fig. 6A).

#### 4. Discussion

This is the first study that reports and quantifies AIs ingestion by the European hake off the Catalan coast (NW Mediterranean) in relation to the exposure of the AIs from the surrounding environment, the near-

bottom water layer. A multidisciplinary approach, as in the present case, offers valuable opportunities to appreciate the simultaneous behaviour of a number of factors of different nature, which is usually complex and difficult to assess.

##### 4.1. Characterization of environmental and ingested AIs

Microplastics studies have demonstrated that a wide range of AIs shapes can be found in the marine environment (Hidalgo-Ruz et al., 2012; Lusher et al., 2017; Hartmann et al., 2019). Present results highlight that fibre-shaped items are the most abundant AIs (i.e. 97.8%) found both in fish digestive tracts and in near-bottom water samples, as has already been proved in several studies from the Mediterranean Sea (Bellas et al., 2016; Compa et al., 2018; Suaria et al., 2020; Rodríguez-Romeu et al., 2020; Carreras-Colom et al., 2020, 2022a, 2022b), making clear that they dominate micro-litter composition in this area, both in fish and near-bottom water.

Given that most of the fibres found in the marine environment are made of cellulose (Avio et al., 2020; Suaria et al., 2020), in the present study non-synthetic polymers (cellulosic-like fibres) have been characterized and quantified in addition to the synthetic polymers. However,



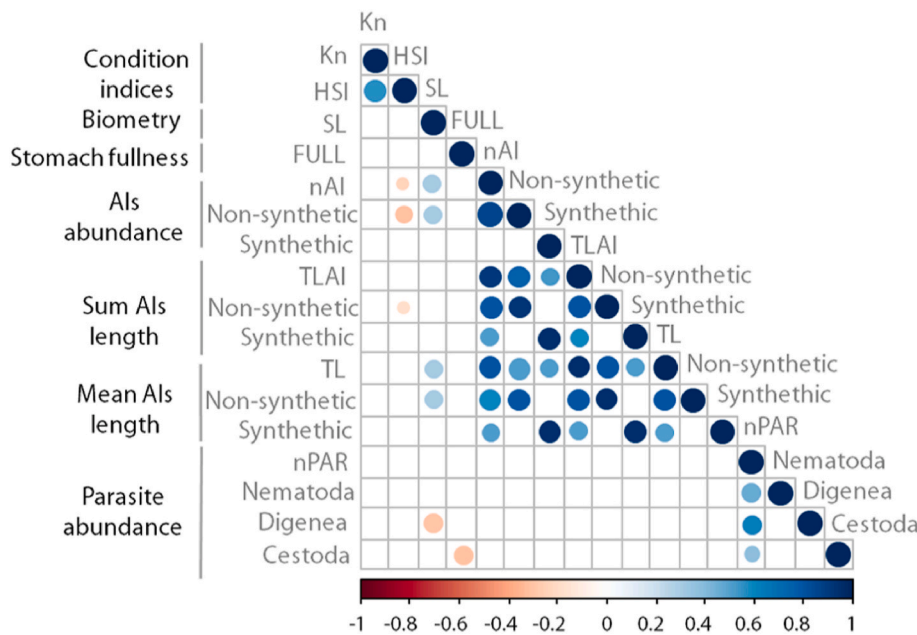


**Fig. 5.** Correlation matrix indicating positive (blue) and negative (red) significant ( $p < 0.05$ ) correlations among total AIs abundance (nAI), non-synthetic fibres (Non-synthetic) and synthetic fibres (Synthetic) abundance, sum of total AIs lengths (TLAI), non-synthetic fibres (Non-synthetic) and synthetic fibres (Synthetic) sum of lengths, mean of total AIs lengths (TL), non-synthetic fibres (Non-synthetic) and synthetic fibres (Synthetic) mean of lengths, fish standard length (SL), stomach fullness (FULL), Le Cren relative condition index (Kn) and hepatosomatic index (HSI), and total abundance of parasites (nPAR), and of main parasite taxa (i.e. nematodes, digeneans and cestodes), found within *Merluccius merluccius* digestive tracts. Circle size and colour intensity are proportional to the value of the correlation coefficient.

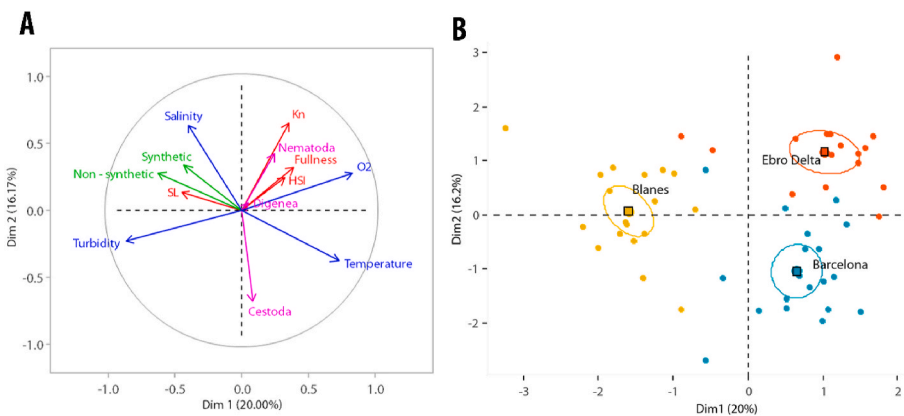


**Fig. 6.** (A) Multiple Factor Analysis (MFA) displaying relationships among AIs abundance (synthetic and non-synthetic) in the hake digestive tract, fish health condition indices (Kn, HSI), stomach fullness and standard length (SL), abundance of main parasite taxa (Nematoda, Digenea and Cestoda) and abiotic conditions measured on the near-bottom water layer (temperature, salinity, turbidity and  $O_2$  concentration). (B) Factor map of the MFA results for *Merluccius merluccius* individuals from each locality. Each individual is represented by a dot.

given that most of the available studies on the subject have only focused on reporting MPs (Hidalgo-Ruz et al., 2012; Hartmann et al., 2019), comparison of present results regarding the total amount of AIs with published data can be inaccurate. Thus, these studies are compared to only the synthetic fibre data. Furthermore, although some studies have excluded non-synthetic fibres from their results to avoid overestimation of AIs due to airborne contamination (Foekema et al., 2013), the present study demonstrates that working on isolation devices can effectively prevent background contamination of the samples and thus provide reliable results. As a matter of fact, several studies focusing on micro-litter and avoiding digestion methods have highlighted a much greater presence of cellulosic fibres both in biotic and abiotic compartments (Sanchez-Vidal et al., 2018; Suaria et al., 2020; Rodríguez-Romeu et al., 2020). For all this, it is of major importance to avoid destructive digestion techniques that can potentially degrade cellulose-based fibres (Dehaut et al., 2016; Kühn et al., 2017; Treilles et al., 2020) and to establish a standardized methodology to characterize micro-debris (Athey and Erdle, 2022).

Most of the AIs ingested by hakes were cellulosic fibres smaller than 5 mm, which corresponds to the traditional microplastic size-based definition. Similar sizes of AIs (<2.6 mm) were found both in the digestive tract of hakes and in the near-bottom water layer off Blanes and Ebro Delta. This result is in accordance with what Bellas et al.

(2016) reported in the digestive tract of hakes from the Gulf of Cadiz (fibres size <3.1 mm). This high abundance of cellulosic fibres found in the present study has indeed been reported in other marine environments such as the deep-sea (Sanchez-Vidal et al., 2018) and inside the digestive tract of other fish and crustacean species (Carreras-Colom et al., 2018, 2020; Rodríguez-Romeu et al., 2020, 2022). Its origin is mainly associated to textile industries and households, from which fibres are released through wastewater treatment plants, or to discharges from domestic washing machines into the seas (Browne et al., 2011). The long-term accumulation of cellulose in the marine environment could be explained by the fact that natural fabrics release more fibres during laundering than synthetics, and although they are considered biodegradable, their degradation rate is poorly understood and may be slowed down if these fibres have been dyed and processed with chemical products (Suaria et al., 2020).

Literature on the abundance of MPs in seawater has highlighted a heterogeneous spatial distribution of marine debris in the Mediterranean Sea (Suaria and Aliani, 2014; Spedicato et al., 2019), which is corroborated by present results, mostly regarding the higher abundance of synthetic AIs in polluted areas (Alomar et al., 2016) such as off Barcelona. Available studies have mostly focused on quantifying MP concentrations from surface waters (Cózar et al., 2015; Suaria et al., 2020) and from the seafloor sediments (Woodall et al., 2014; Sanchez-Vidal

et al., 2018). Few studies regarding their vertical distribution have demonstrated that, due to their properties, which include shape, density and chemical composition, most MPs are likely to spread into deeper layers of the water column, where they can interact with marine biota (Reisser et al., 2015; Avio et al., 2020).

Due to the limited number of studies characterizing AIs in the near-bottom water layer in the Mediterranean Sea, comparisons with other data from close regions are difficult to establish. However, taking into consideration only synthetic AIs in order to compare present outcomes with those of other studies carried out in the Mediterranean area, similar AIs concentrations to those observed off Blanes have been detected by Bainsi et al. (2018) in the north Tyrrhenian Sea (0.22 (SD = 0.57) items/m<sup>3</sup>), and by Lefebvre et al. (2019) in the Gulf of Lions (0.23 (SD = 0.20) items/m<sup>3</sup>), whose samplings were performed at different depths of the water column.

Further research should be done in quantifying the abundance of micro-debris in different layers of the water column to better understand the behaviour and fate of these pollutants. For this purpose, it is important to consider the factors that can determine the distribution of AIs in the environment such as urbanization, industry, river inputs, different strategies of wastewater treatment plants, fishing activities, local pollution sources, density properties of micro-debris and resuspension processes likely caused by bottom-trawl fishing vessels (Paradis et al., 2018). Furthermore, the observed differences among localities in AIs concentration from water samples could also be explained by the different morphology of the associated continental shelves. Indeed, the depositional continental shelf off Barcelona, characterized by a smooth bathymetry, is influenced by the Llobregat and Besós rivers that drain densely urbanized areas, and thus discharge huge amounts of AIs, compared to the other two localities, that can easily be accumulated there (Durán et al., 2014). In the case off Blanes, the nearby submarine canyon could have a role in the AIs that arrive from inland sources and probably accumulate them in the deep sea (Tubau et al., 2015). Regarding the area off Ebro Delta, the low abundance of AIs/m<sup>3</sup> detected in water samples suggests that this sampling area might not receive the direct influence of Ebro river discharge and consequently a low land-based AIs input, due to its distance from the coast compared to the other areas. Besides, in this microtidal and low-energy continental shelf, resuspension processes are rare (Palanques et al., 2002), so AIs could sediment more rapidly and thus would not be detected at the near-bottom water. In fact, this is in accordance with the turbidity levels recovered from the present study, which were lower compared to the other two sampling areas (Table S2).

In the present study, hakes captured off the Catalan coast seem to be easily exposed to the ingestion of AIs due to the frequent presence of these elements within their digestive tracts. Similar prevalence values of ingested synthetic AIs in Barcelona and Ebro Delta were reported by Bellas et al. (2016) in hakes from the Gulf of Cadiz (16.7%), but higher mean abundances of AIs per individual were detected in this case (1 AIs/ind) compared to what is reported in the present work (see Table 2). Although hakes from off Blanes presented the highest prevalence and abundance of ingested synthetic AIs in the present study, these values are, by far, lower than what was reported on hakes from the Tyrrhenian Sea (82.5%) (Bianchi et al., 2020), from the Ionian Sea (48%, 1.75 (SD = 2) AIs/ind) and from the Adriatic Sea (30.6%, 1.09 (SD = 0.30) AIs/ind) (Giani et al., 2019), probably due to the different impacts of human activity on the sampling areas and to the different methodology used for AIs quantification.

Considering only fibres, differences in the levels of ingested fibres have also been detected among distinct fish species captured in the same or close to the sampling areas as those considered in the present study: higher levels of ingested fibres were detected in benthic species (Rodríguez-Romeu et al., 2020) compared to the present results, but similar or even lower levels were recorded from pelagic species (Compa et al., 2018; Pennino et al., 2020; Rodríguez-Romeu et al., 2022). These differences could be explained by different fish feeding modes or by the

heterogeneous distribution of AIs in the water column (Bour et al., 2018).

Furthermore, AIs have been impacting the area off Barcelona for the past few years, as our results indicate, since AIs ingested by hakes from 2007 have remained at a similar level as in 2019. Previous studies in the same area detected similar levels of AIs when compared to those ingested in 2007 and 2018 in fish and crustaceans, but reported differences in polymer composition between these two years, highlighting a shift in production and usage trends of textile polymers (Carreras-Colom et al., 2020; Rodríguez-Romeu et al., 2020, 2022). However, considering that local effects on AIs dynamics may exist in this area, no clear evidence of temporal trends for the levels of AIs could be drawn from the present results.

#### 4.2. Comparison between environmental and ingested AIs

For a complete and contextualized interpretation of the levels of AIs ingested by hakes, it is important to take into account the abundance and distribution of plastic debris present in the associated environment. It has been demonstrated that higher concentrations of micro-debris in marine ecosystems from impacted areas imply that fish and other local organisms are easily exposed to them, with the consequent active or passive ingestion of these particles while feeding (Fossi et al., 2018), foraging or drinking (Roch et al., 2020).

Although some studies have detected a clear relationship between the levels of AIs ingested by marine species and their proximity to highly anthropized areas (Andrady, 2011; Giani et al., 2019; Rodríguez-Romeu et al., 2020), in the present study, lower levels of ingested AIs were found off Barcelona, a densely populated coastal area with high concentrations of AIs in the environment. However, these inconsistent results could be explained by the size distribution of fibres from the environment and by the particular feeding behaviour of hakes.

Ontogenetic shifts in the feeding behaviour and diet in juvenile hakes allow the transition from an opportunistic feeding behaviour based on euphausiids, mysids and decapods crustaceans (Modica et al., 2011) to a more selective foraging behaviour (D'Iglio et al., 2022) dominated by small and fast-moving fishes and suprabenthic crustaceans of the sub-order Gammaridea, the orders Mysidacea, Euphausiacea and natantian decapods (Carrassón et al., 2019). This high specialization on certain prey in hakes from sizes as those in the present study, could be related to a low probability of ingesting large fibres from their surrounding environment.

In fact, according to present results, the size and polymer composition of ingested fibres were similar to those of fibres from the environment off Blanes and Ebro Delta. However, in Barcelona the fibre size distribution from water samples was much wider than that of fibres ingested by hakes due to the predominance of extra-large polyamide fibres in the environment, which were absent in the fish digestive tracts. Considering only the total abundance of fibres within the observed size range of ingested AIs for hakes, the concentration of AIs in Barcelona would be reduced from 1.53 to 0.26 items/m<sup>3</sup>, a lower value than the concentration of AIs from the other two localities, but consistent with the lower levels of AIs ingested by hakes from this area. Thus, hakes could overcome the exposure to large fibres, and only ingest accidentally those below a certain size threshold.

To sum up, for a mean of 0.85 items/m<sup>3</sup> of AIs from the surrounding water from the three localities considered together, examined fish ingested 1.39 (SD = 1.39) items/individual. However, important differences, due to the high differences in the size range of environmental AIs depending on the sampling station, were observed at a local scale. Overall, levels of micro-debris detected both in the environment and ingested by hakes are consistent for fibres below 6 mm size, indicating that this species could be useful as a bioindicator species for monitoring small-sized micro-debris present in the near-bottom water layer.

### 4.3. Association of ingested AIs to hake health status

Present results suggest that ingested AIs do not significantly affect in a negative way the general health condition, nutritional state or feeding activity of *M. merluccius*, since no association with condition indices or stomach fullness was detected. Similar outcomes have been reported in other fish species like *Sardina pilchardus*, *Engraulis encrasicolus* (Compa et al., 2018; Rodríguez-Romeu et al., 2022) and *Mullus barbatus* (Rodríguez-Romeu et al., 2020).

Negative effects related to AIs ingestion on fish health have been described in experimental studies working with acute exposures to high levels of MPs (Kögel et al., 2020). At the histopathological level, the mucosa of the digestive tract is expected to be affected due to its direct contact with the AIs. In fact, intestinal damage and inflammatory changes were detected in *Sparus aurata* exposure study with 100–500 mg of microparticles (with sizes ranging between 40 and 150 µm) per kg of feed (Espinosa et al., 2017; Kögel et al., 2020). Also, an increase in rodlet cells abundance in the intestinal mucosa of *Dicentrarchus labrax* was noticed in exposure experiments with diets containing 0.1% (w/w) of MPs for 90 days (Pedà et al., 2016). However, these outcomes are hardly comparable to patterns observed in the natural environment, where concentrations of AIs are much lower. In the wild, no consistent effects on health condition have been found in *Aristeus antennatus* (Carreras-Colom et al., 2018), *M. barbatus* (Rodríguez-Romeu et al., 2020) nor *E. encrasicolus* (Rodríguez-Romeu et al., 2022). Similar to these later studies, in the case of *M. merluccius*, AIs seem to pass through the digestive tract in the same way as digested prey contents since no significant differences were detected between the abundance of AIs from the stomach and intestine. Besides, no alterations in the digestive tract potentially associated with AIs were noticed which is in accordance with other studies (Jovanović, 2017; Jovanović et al., 2018; Batel et al., 2020). Although rodlet cells have been reported as immune cells and biomarkers of exposure to contaminants, such as MPs (Pedà et al., 2016), their origin and function are still controverted (Manera and Dezfuli, 2004), and in the present study their presence is not associated with AIs abundance.

Although some studies have detected MPs in the liver or muscle (Collard et al., 2017; Haave et al., 2021), the processes by which MPs from the digestive system could be translocated into other organs are not yet demonstrated and well understood as methodological limitations prevent the precise localization of MPs within the organs (Burns and Boxall, 2018). AIs found in this study are unlikely to pass through the intestinal barrier due to their size (Burns and Boxall, 2018), but potentially toxic additives and substances that could be present in the AIs (Amelia et al., 2021), can be released and absorbed in the intestine, and therefore could reach other organs, such as the liver. Some experimental studies have recorded some alterations detected in the liver which include decreased energy storage of glycogen (Rochman et al., 2013), effects on lipid tissues, inflammation (Lu et al., 2016), oxidative damage and necrosis (Chen et al., 2017). However, the findings found in the liver sections in the present study are not correlated with the presence or levels of AIs, so they are probably associated with natural metabolic changes related to different feeding regimes and/or by the presence of nematode parasites. This is not surprising considering that studies finding tissue alterations associated with MPs have been conducted using very high levels of MPs, much higher than the levels detected in this study.

No clear trends were found between the abundance of parasites with fish size or condition indices nor with AIs ingestion. So, parasites seem not to interfere in the accumulation of AIs within the digestive tract, as reported by Rodríguez-Romeu et al. (2020). This contrasts with what Hernandez-Milian et al. (2019) suggested in grey seals. Recently, Penino et al. (2020) reported a positive relationship between MPs and parasites in anchovies, and explained their results on the basis that individuals from more polluted areas ingested more MPs and thus, were more likely to be infected by parasites. However, further research would

be needed to assess the potential relationship between MPs and parasite aggregations.

Differences found in Kn and HSI values among localities could be related to the variability regarding food availability and environmental conditions such as temperature or oxygen concentration, which are regarded as the most important factors impacting fish health (Lloret et al., 2014). The significantly higher values of Kn and HSI observed in the individuals from off Ebro Delta could be related to a higher oxygen concentration and to a greater quantity and/or availability of prey in this locality linked to a higher food consumption, as demonstrated by the higher values of the fullness index (yet not significant) in this locality, which could enhance the general condition of hakes in this area (Hidalgo et al., 2008). Moreover, Lloret et al. (2002) reported that individuals inhabiting shallower habitats, as in the case of Ebro Delta, were in better condition than those in deeper waters given that shallow areas are important habitats for food resources. Nevertheless, individuals from off Barcelona were in a poorer condition compared to individuals from the other two localities. Although individuals in this area were slightly more parasitized than in other areas, no significant correlations were found between condition indices and parasite indicators. It could be hypothesized that certain environmental conditions or factors related to anthropogenic pollution affecting this area could cause a detrimental impact on fish condition.

## 5. Conclusions

The present study demonstrates the widespread presence of AIs in the near-bottom water layer and their ingestion by *M. merluccius* off the Catalan coast (NW Mediterranean Sea). Barcelona was the sampling point with the greatest abundance of AIs present in the environment, however, the total abundance of AIs ingested by hakes (determined by AIs size range) was lower than in the other localities, probably due to the feeding behaviour of juvenile hakes, which is paramount to take into account in marine litter studies. The most abundant type of AIs found were cellulosic fibres despite the predominant abundance of large polyamide fibres in the water samples from off Barcelona. No potential impact of AIs could be detected by fish condition indices, histological assessment or parasitological descriptors. Despite this, it is essential to keep developing tools to accurately assess plastic pollution's impact on ecosystems so that potential harmful effects can be detected and evaluated as early as possible.

### CRedit authorship contribution statement

**Laura Muns-Pujadas:** Methodology, Formal analysis, Investigation, Writing – original draft, Writing – review & editing, Visualization. **Sara Dallarés:** Methodology, Investigation, Writing – original draft, Writing – review & editing, Supervision. **Maria Constenla:** Conceptualization, Methodology, Investigation, Writing – review & editing, Supervision. **Francesc Padrós:** Conceptualization, Methodology, Investigation, Writing – review & editing, Supervision. **Ester Carreras-Colom:** Methodology, Investigation, Writing – review & editing. **Michaël Grelaud:** Methodology, Investigation, Resources, Writing – review & editing, Funding acquisition. **Maitte Carrassón:** Conceptualization, Methodology, Investigation, Resources, Writing – original draft, Writing – review & editing, Supervision, Project administration, Funding acquisition. **Anna Soler-Membrives:** Conceptualization, Methodology, Formal analysis, Investigation, Writing – original draft, Writing – review & editing, Supervision.

### Declaration of competing interest

The authors declare that they have no known competing financial interests or personal relationships that could have appeared to influence the work reported in this paper.

## Data availability

Data will be made available on request.

## Acknowledgements

This work was supported by the Spanish Ministry of Science and Technology “BIOMARE” project (CTM2006-13508-C02-01MAR), by the Spanish Ministry of Science, Innovation and Universities “PLASMAR” project (RTI 2018-094806-B-100) and i-plastic project (JPI-Oceans—Grant PCI2020-112059). We thank all fishermen from commercial fishing vessels involved in the “BIOMARE” and “PLASMAR” projects. L. M-P. benefits from an FI-DGR Ph.D. student grant from the Generalitat de Catalunya (2022 FI\_B 00405). M.G. acknowledges financial support from the i-plastic project (JPI-Oceans—Grant PCI 2020-112059). E.C.-C. acknowledges financial support from European Union NextGenerationEU.

## Appendix A. Supplementary data

Supplementary data to this article can be found online at <https://doi.org/10.1016/j.marenvres.2023.105921>.

## References

- Alomar, C., Estarellas, F., Deudero, S., 2016. Microplastics in the Mediterranean sea: deposition in coastal shallow sediments, spatial variation and preferential grain size. *Mar. Environ. Res.* 115, 1–10. <https://doi.org/10.1016/j.marenvres.2016.01.005>.
- Amelia, T.S.M., Khalik, W.M.A.W.M., Ong, M.C., Shao, Y.T., Pan, H.-J., Bhupalan, K., 2021. Marine microplastics as vectors of major ocean pollutants and its hazards to the marine ecosystem and humans. *Prog. Earth Planet. Sci.* 8, 12. <https://doi.org/10.1186/s40645-020-00405-4>.
- Andrady, A.L., 2011. Microplastics in the marine environment. *Mar. Pollut. Bull.* 62 (8), 1596–1605. <https://doi.org/10.1016/j.marpolbul.2011.05.030>.
- Arthur, C., Baker, J., Bamford, H., 2009. *Proceedings of the International Research Workshop on the Occurrence, Effects and Fate of Microplastic Marine Debris*. NOAA Technical Memorandum NOS-OR&R30. Sept 9–11, 2008.
- Athey, S.N., Erdle, L.M., 2022. Are we underestimating anthropogenic microfiber pollution? A critical review of occurrence, methods, and reporting. *Environ. Toxicol. Chem.* 41, 822–837. <https://doi.org/10.1002/etc.5173>.
- Au, D.W.T., 2004. The application of histo-cytopathological biomarkers in marine pollution monitoring: a review. *Mar. Pollut. Bull.* 48, 817–834. <https://doi.org/10.1016/j.marpolbul.2004.02.032>.
- Avio, C.G., Pittura, L., D’Errico, G., Abel, S., Amorello, S., Marino, G., Gorb, S., Regoli, F., 2020. Distribution and characterization of microplastic particles and textile microfibrils in Adriatic food webs: general insights for biomonitoring strategies. *Environ. Pollut.* 258, 113766. <https://doi.org/10.1016/j.envpol.2019.113766>.
- Baini, M., Fossi, M.C., Galli, M., Caliana, I., Campania, T., Finoia, M.G., Panti, C., 2018. Abundance and characterization of microplastics in the coastal waters of Tuscany (Italy): the application of the MSFD monitoring protocol in the Mediterranean Sea. *Mar. Pollut. Bull.* 133, 543–552. <https://doi.org/10.1016/j.marpolbul.2018.06.016>.
- Batel, A., Baumann, L., Carteny, C.C., Cormier, B., Keiter, S.H., Braunbeck, T., 2020. Histological, enzymatic and chemical analyses of the potential effects of differently sized microplastic particles upon long-term ingestion in zebrafish (*Danio rerio*). *Mar. Pollut. Bull.* 153. <https://doi.org/10.1016/j.marpolbul.2020.111022>.
- Bellas, J., Martínez-Armental, J., Martínez-Cámara, A., Besada, V., Martínez-Gómez, C., 2016. Ingestion of microplastics by demersal fish from the Spanish Atlantic and Mediterranean coasts. *Mar. Pollut. Bull.* 109, 55–60. <https://doi.org/10.1016/j.marpolbul.2016.06.026>.
- Bianchi, J., Valente, T., Scacco, U., Cimmaruta, R., Sbrana, A., Silvestri, C., Matiddi, M., 2020. Food preference determines the best suitable digestion protocol for analysing microplastic ingestion by fish. *Mar. Pollut. Bull.* 154, 111050. <https://doi.org/10.1016/j.marpolbul.2020.111050>.
- Bour, A., Avio, C.G., Gorb, S., Regoli, F., Hylland, K., 2018. Presence of microplastics in benthic and epibenthic organisms: influence of habitat, feeding mode and trophic level. *Environ. Pollut.* 243, 1217–1225. <https://doi.org/10.1016/j.envpol.2018.09.115>.
- Bozzano, A., Recasens, L., Sartor, P., 1997. Diet of the European hake *Merluccius merluccius* (pisces: merlucciidae) in the western mediterranean (Gulf of Lions). *Sci. Mar.* 61, 1–8.
- Browne, M.A., Crump, P., Niven, S.J., Teuten, E., Tonkin, A., Galloway, T., Thompson, R., 2011. Accumulation of microplastic on shorelines worldwide: sources and sinks. *Environ. Sci. Technol.* 45, 9175–9179. <https://doi.org/10.1021/es201811s>.
- Burns, E.E., Boxall, A.B.A., 2018. Microplastics in the aquatic environment: evidence for or against adverse impacts and major knowledge gaps. *Environ. Toxicol. Chem.* 37, 2776–2796. <https://doi.org/10.1002/etc.4268>.
- Bush, A.O., Lafferty, K.D., Lotz, J.M., Shostak, A.W., 1997. Parasitology meets ecology on its own terms: margolis et al. Revisited. *J. Parasitol.* 83, 575. <https://doi.org/10.2307/3284227>.
- Carpenter, E.J., Smith, K.L., 1972. Plastics on the sargasso sea surface. *Science* 175, 1240–1241. <https://doi.org/10.1126/science.175.4027.1240>.
- Carrasón, M., Dallarés, S., Cartes, J.E., Constenla, M., Pérez-del-Olmo, A., Zucca, L., Kostadinova, A., 2019. Drivers of parasite community structure in fishes of the continental shelf of the Western Mediterranean: the importance of host phylogeny and autecological traits. *Int. J. Parasitol.* 49 (9), 669–683. <https://doi.org/10.1016/j.ijpara.2019.04.004>.
- Carreras-Colom, E., Constenla, M., Soler-Membrives, A., Cartes, J.E., Baeza, M., Padrós, F., Carrasón, M., 2018. Spatial occurrence and effects of microplastic ingestion on the deep-water shrimp *Aristeus antennatus*. *Mar. Pollut. Bull.* 133, 44–52. <https://doi.org/10.1016/j.marpolbul.2018.05.012>.
- Carreras-Colom, E., Constenla, M., Soler-Membrives, A., Cartes, J.E., Baeza, M., Carrasón, M., 2020. A closer look at anthropogenic fiber ingestion in *Aristeus antennatus* in the NW Mediterranean Sea: differences among years and locations and impact on health condition. *Environ. Pollut.* 263, 114567. <https://doi.org/10.1016/j.envpol.2020.114567>.
- Carreras-Colom, E., Cartes, J.E., Constenla, M., Welden, N.A., Soler-Membrives, A., Carrasón, M., 2022a. An affordable method for monitoring plastic fibre ingestion in *Nephrops norvegicus* (Linnaeus, 1758) and implementation on wide temporal and geographical scale comparisons. *Sci. Total Environ.* 810, 152264. <https://doi.org/10.1016/j.scitotenv.2021.152264>.
- Carreras-Colom, E., Cartes, J.E., Rodríguez-Romeu, O., Padrós, F., Solé, M., Grelaud, M., Ziveri, P., Palet, C., Soler-Membrives, A., Carrasón, M., 2022b. Anthropogenic pollutants in *Nephrops norvegicus* (Linnaeus, 1758) from the NW Mediterranean Sea: uptake assessment and potential impact on health. *Environ. Pollut.* 314, 120230. <https://doi.org/10.1016/j.envpol.2022.120230>.
- Cartes, J.E., Rey, J., Lloris, D., Gil De Sola, L., 2004. Influence of environmental variables on the feeding and diet of European hake (*Merluccius merluccius*) on the Mediterranean Iberian coasts. *J. Mar. Biol. Assoc. U. K.* 84, 831–835. <https://doi.org/10.1017/S0025315404010021h>.
- Chen, Q.Q., Gundlach, M., Yang, S.Y., Jiang, J., Velki, M., Yin, D.Q., Hollert, H., 2017. Quantitative investigation of the mechanisms of microplastics and nanoplastics toward zebrafish larvae locomotor activity. *Sci. Total Environ.* 584, 1022–1031. <https://doi.org/10.1016/j.scitotenv.2017.01.156>.
- Cole, M., Lindeque, P., Halsband, C., Galloway, T.S., 2011. Microplastics as contaminants in the marine environment: a review. *Mar. Pollut. Bull.* 62 (12), 2588–2597. <https://doi.org/10.1016/j.marpolbul.2011.09.025>.
- Cole, M., Webb, H., Lindeque, P.K., Fileman, E.S., Halsband, C., Galloway, T.S., 2014. Isolation of microplastics in biota-rich seawater samples and marine organisms. *Sci. Rep.* 4, 4528. <https://doi.org/10.1038/srep04528>.
- Collard, F., Gilbert, B., Compère, P., Eppe, G., Das, K., Jauniaux, T., Parmentier, E., 2017. Microplastics in livers of European anchovies (*Engraulis encrasicolus*, L.). *Environ. Pollut.* 229, 1000–1005. <https://doi.org/10.1016/j.envpol.2017.07.089>.
- Compa, M., Ventero, A., Iglesias, M., Deudero, S., 2018. Ingestion of microplastics and natural fibres in *Sardina pilchardus* (Walbaum, 1792) and *Engraulis encrasicolus* (Linnaeus, 1758) along the Spanish Mediterranean coast. *Mar. Pollut. Bull.* 128, 89–96. <https://doi.org/10.1016/j.marpolbul.2018.01.009>.
- Cowger, W., Booth, A.M., Hamilton, B.M., Thaysen, C., Primpke, S., Munno, K., Lusher, A.L., Dehaut, A., Vaz, V.P., Liboiron, M., Devriese, L.L., Hermabessiere, L., Rochman, C., Athey, S.N., Lynch, J.M., De Frond, H., Gray, A., Jones, O.A.H., Brander, S., Steele, C., Moore, S., Sanchez, A., Nel, H., 2020. Reporting guidelines to increase the reproducibility and comparability of research on microplastics. *Appl. Spectrosc.* 74, 1066–1077. <https://doi.org/10.1017/0003702820930292>.
- Cózar, A., Sanz-Martín, M., Martí, E., González-Gordillo, J.I., Ubeda, B., Gálvez, J.Á., Irigoien, X., Duarte, C.M., 2015. Plastic accumulation in the Mediterranean Sea. *PLoS One* 10, e0121762. <https://doi.org/10.1371/journal.pone.0121762>.
- de Haan, W.P., Sanchez-Vidal, A., Canals, M., 2019. Floating microplastics and aggregate formation in the western Mediterranean Sea. *Mar. Pollut. Bull.* 140, 523–535. <https://doi.org/10.1016/j.marpolbul.2019.01.053>.
- Dehaut, A., Cassone, A.L., Frère, L., Hermabessiere, L., Himber, C., Rinnert, E., Rivière, G., Lambert, C., Soudant, P., Huvet, A., Duflos, G., Paul-Pont, I., 2016. Microplastics in seafood: benchmark protocol for their extraction and characterization. *Environ. Pollut.* 215, 223–233. <https://doi.org/10.1016/j.envpol.2016.05.018>.
- D’Iglio, C., Porcino, N., Savoca, S., Profeta, A., Perdichizzi, A., Mincicante, E.A., Salvati, D., Soraci, F., Rinelli, P., Giordano, D., 2022. Ontogenetic shift and feeding habits of the European hake (*Merluccius merluccius* L., 1758) in Central and Southern Tyrrhenian Sea (Western Mediterranean sea): a comparison between past and present data. *Ecol. Evol.* 12, e8634. <https://doi.org/10.1002/ece3.8634>.
- Durán, R., Canals, M., Sanz, J.L., Lastras, G., Amblas, D., Micallef, A., 2014. Morphology and sediment dynamics of the northern Catalan continental shelf, northwestern Mediterranean Sea. *Geomorphology* 204, 1–20. <https://doi.org/10.1016/j.geomorph.2012.10.004>.
- Eriksen, M., Lebreton, L.C.M., Carson, H.S., Thiel, M., Moore, C.J., Borerro, J.C., Galgani, F., Ryan, P.G., Reisser, J., 2014. Plastic pollution in the world’s oceans: more than 5 trillion plastic pieces weighing over 250,000 tons afloat at sea. *PLoS One* 9, e111913. <https://doi.org/10.1371/journal.pone.0111913>.
- Espinosa, C., Cuesta, A., Esteban, M.A., 2017. Effects of dietary polyvinylchloride microparticles on general health, immune status and expression of several genes related to stress in gilthead seabream (*Sparus aurata* L.). *Fish Shellfish Immunol.* 68, 251–259. <https://doi.org/10.1016/j.fsi.2017.07.006>.



- Taylor, M.L., Gwinnett, C., Robinson, L.F., Woodall, L.C., 2016. Plastic microfibre ingestion by deep-sea organisms. *Sci. Rep.* 6 (1) <https://doi.org/10.1038/srep33997>.
- Thompson, R.C., 2015. Microplastics in the marine environment: sources, consequences and solutions. In: Bergmann, M., Gutow, L., Klages, M. (Eds.), *Marine Anthropogenic Litter*. Springer, Cham. [https://doi.org/10.1007/978-3-319-16510-3\\_7](https://doi.org/10.1007/978-3-319-16510-3_7).
- Torre, M., Digka, N., Anastasopoulou, A., Tsangaris, C., Mytilineou, C., 2016. Anthropogenic microfibres pollution in marine biota. A new and simple methodology to minimize airborne contamination. *Mar. Pollut. Bull.* 113, 55–61. <https://doi.org/10.1016/j.marpolbul.2016.07.050>.
- Treilles, R., Cayla, A., Gasperi, J., Strich, B., Ausset, P., Tassin, B., 2020. Impacts of organic matter digestion protocols on synthetic, artificial and natural raw fibers. *Sci. Total Environ.* 748, 141230 <https://doi.org/10.1016/j.scitotenv.2020.141230>.
- Tubau, X., Canals, M., Lastras, G., Rayo, X., Rivera, J., Amblas, D., 2015. Marine litter on the floor of deep submarine canyons of the Northwestern Mediterranean Sea: the role of hydrodynamic processes. *Prog. Oceanogr.* 134, 379–403. <https://doi.org/10.1016/j.pocean.2015.03.013>.
- UNEP/MAP, 2015. *Marine Litter Assessment in the Mediterranean*. Athens, Greece.
- van Sebille, E., Aliani, S., Law, K.L., Maximenko, N., Alsina, J.M., Bagaev, A., Bergmann, M., Chapron, B., Chubarenko, I., Cozar, A., Delandmeter, P., Egger, M., Fox-Kemper, B., Garaba, S.P., Goddijn-Murphy, L., Hardesty, B.D., Hoffman, M.J., Isobe, A., Jongedijk, C.E., Kaandorp, M.L.A., Khatmullina, L., Koelmans, A.A., Kukulka, T., Laufkotter, C., Lebreton, L., Lobelle, D., Maes, C., Martinez Vicente, V., Maqueda, M.A.M., Poulain-Zarcos, M., Rodriguez, E., Ryan, P.G., Shanks, A.L., Shim, W.J., Suaria, G., Thiel, M., van den Bremer, T.S., Wichmann, D., 2020. The physical oceanography of the transport of floating marine debris. *Environ. Res. Lett.* 15 (2), 32. <https://doi.org/10.1088/1748-9326/ab6d7d>.
- Vidal-Martínez, V.M., Pech, D., Sures, B., Purucker, S.T., Poulin, R., 2010. Can parasites really reveal environmental impact? *Trends Parasitol.* 26 (1), 44–51. <https://doi.org/10.1016/j.pt.2009.11.001>.
- Woodall, L.C., Sanchez-Vidal, A., Canals, M., Paterson, G.L.J., Coppock, R., Sleight, V., Calafat, A., Rogers, A.D., Narayanaswamy, B.E., Thompson, R.C., 2014. The deep sea is a major sink for microplastic debris. *R. Soc. Open Sci.* 1 <https://doi.org/10.1098/rsos.140317>, 140317-140317.
- Zhu, X., Nguyen, B., You, J.B., Karakolis, E., Sinton, D., Rochman, C., 2019. Identification of microfibers in the environment using multiple lines of evidence. *Environ. Sci. Technol.* 53, 11877–11887. <https://doi.org/10.1021/acs.est.9b05262>.